Finite f-electron bandwidth in a heavy-fermion model

A. Euverte,[1] S. Chiesa,[2] R. T. Scalettar,[3] and G. G. Batrouni[1,4,5]

[1]*INLN, Université de Nice-Sophia Antipolis, CNRS, 1361 route des Lucioles, 06560 Valbonne, France*

[2]*Department of Physics, College of William & Mary, Williamsburg, Virginia 23185, USA*

[3]*Physics Department, University of California, Davis, California 95616, USA*

[4]*Institut Universitaire de France, 103 boulevard Saint-Michel, 75005 Paris, France*

[5]*Centre for Quantum Technologies, National University of Singapore, 2 Science Drive 3, Singapore 117542*

(Received 1 October 2013; revised manuscript received 23 November 2013; published 20 December 2013)

The determinant quantum Monte Carlo (DQMC) method is used to study the effect of nonzero hopping t_f in the "localized" f band of the periodic Anderson model (PAM) in two dimensions. The low-temperature properties are determined in the plane of interband hybridization V and t_f at fixed U_f and half filling, including the case when the sign of t_f is opposite to that of the conduction band t_d. For t_f and t_d of the same sign and when $t_f/t_d > (V/4t_d)^2$, the noninteracting system is metallic. We show that a remnant of the band insulator to metal line at $U_f = 0$ persists in the interacting system, manifesting itself as a maximal tendency toward antiferromagnetic correlations at low temperature. In this "optimal" t_f region, short-range (e.g., near-neighbor) and long-range spin correlations develop at similar temperatures and have comparable magnitude. Both observations are in stark contrast to the situation in the widely studied PAM ($t_f = 0$) and single-band Hubbard model, where short-range correlations are stronger and develop at higher temperature. The effect that finite t_f has on Kondo screening is investigated by considering the evolution of the local density of states for selected t_f as a function of V. We use mean-field theory as a tool to discriminate those aspects of the physics that are genuinely many-body in character.

DOI: 10.1103/PhysRevB.88.235123 PACS number(s): 75.30.Mb, 71.27.+a, 71.10.Fd, 75.10.Jm

I. INTRODUCTION

The single-band Hubbard Hamiltonian is the simplest itinerant electron model used to describe the effects of strong correlation in solids.[1–4] At half filling and at low temperatures, an on-site repulsion U drives the emergence of a Mott insulator (MI) phase as well as, on bipartite lattices, antiferromagnetic (AF) correlations. Upon doping, mobile defects are introduced into this MI, and the Hubbard model exhibits more exotic correlation effects, including, in two dimensions, incommensurate charge and spin correlations ("striped phases")[5–9] and, very possibly, d-wave superconductivity.[10]

Some fundamental correlation physics, however, is best considered within multiband Hamiltonians. The periodic Anderson model (PAM),[4] for example, describes the competition of antiferromagnetic order and singlet formation in which highly correlated electrons in one "f" orbital are screened by weakly correlated electrons in a second "d" orbital. These two possible ground states in the PAM are thought to describe qualitatively the observation that certain f-electron systems like $CeAl_2$ are antiferromagnetic, while others like $CeAl_3$ are not, and also to be relevant to materials in which AF is lost (and superconductivity appears) as pressure is applied and the ratio of correlation to kinetic energies is decreased.[11] The "heavy-fermion"[12] behavior in such rare-earth materials, in which the electrons acquire a large effective mass, is also a feature of the PAM. Some physics which was believed to be specific to the PAM, notably the appearance of a Kondo resonance in the density of states, is now known to occur in single-band models as well.[13–16]

Indeed, analytic and numerical investigations have shown that the AF-singlet competition is rather generic. That is, it occurs in a variety of other two-band models, not just ones in which the f band is completely localized, $t_f = 0$. Perhaps the most straightforward alternative to the two-dimensional PAM is the two-band (or two-layer) Hubbard Hamiltonian, in which the intralayer hopping and interaction strengths are chosen to be identical (i.e., $t_f = t_d$ and $U_f = U_d$). Although there is initially a greater AF tendency than in a single layer as the interlayer hybridization V grows toward $V = t_f$, this is followed by a rather rapid decrease of magnetization and the eventual loss of long-range order when $V \simeq 1.6t_f$.[17] This AF to paramagnetic (singlet) transition is also present in quantum spin models like the two-layer Heisenberg model[18] and in Hubbard and Heisenberg ladders.[19]

The goal of the present paper is to obtain a more systematic picture of the nature of the AF-singlet competition and related aspects of Kondo physics at finite temperature.[20] Specifically, we consider a two-orbital model in which t_f interpolates smoothly between the well-known PAM ($t_f = 0$) and the equal bandwidth ($t_f = t_d$) cases. We also study $t_f < 0$, a regime in which, as at $t_f = 0$, the system is a band insulator in the absence of interactions. A particularly interesting issue is the interplay of the Ruderman-Kittel-Kasuya-Yosida (RKKY) interactions, in which the f moments couple indirectly through the conduction bands, and direct exchange $J \sim t_f^2/U_f$. Both give rise to antiferromagnetic correlations, yet we show that their joint effects do not manifest as a straightforward reinforcement. One origin of the complexity is that while V increases the RKKY AF tendency, it also affects the band structure in the localized f band and hence the density of states there. This latter effect is captured by the Stoner criterion in a mean-field treatment.

Allowing a finite bandwidth in the f band makes the PAM a more realistic model for describing heavy-fermion materials. In the case of actinides,[21] the ratio of the interband hybridization over the f-band nearest-neighbor hopping has been recently estimated to be of the order of $V/t_f \approx 3$. Several papers have considered similar models,[22–26] but the effect of t_f has been systematically explored only in the

infinite-dimension case[23] using dynamical mean-field theory (DMFT). For example, de' Medici *et al.*[25] have focused on the closing of the Mott gap with increasing t_f and how this insulator-metal transition differs at zero and finite temperature. We will show that accounting for magnetism leads to different conclusions from the mere renormalization of the noninteracting density of states found by DMFT.[23]

Although our focus is on the magnetic correlations and spectral function in the f band, our results connect also to work which explores the question of "orbitally selective" Mott transitions.[27–38] Here two-band Hamiltonians with different U_f and U_d that are coupled by either interorbital hybridization (as in the present paper) or interactions are solved. The key issue is whether the two fermionic species can be of mixed character, with one being metallic and one insulating.

The remainder of this paper is organized as follows: In Sec. II, we write down the model Hamiltonian to be examined and briefly summarize the mean-field theory (MFT) and the determinant quantum Monte Carlo (DQMC) formalisms. Section III presents MFT and DQMC results for magnetic correlations, while Sec. IV gives those for the local spectral function in the correlated band. The summary and conclusions are in Sec. V.

II. MODEL AND CALCULATIONAL METHODS

The two-band fermionic Hubbard Hamiltonian we consider here,

$$\hat{\mathcal{H}} = -\sum_{\langle \mathbf{j},\mathbf{k}\rangle l\sigma} t_l\,(c^\dagger_{\mathbf{j}l\sigma}c_{\mathbf{k}l\sigma} + \text{H.c.}) - V\sum_{\mathbf{j},\sigma}(c^\dagger_{\mathbf{j}f\sigma}c_{\mathbf{j}d\sigma} + \text{H.c.}) + \sum_{\mathbf{j}l} U_l\left(n^\uparrow_{\mathbf{j}l} - \frac{1}{2}\right)\left(n^\downarrow_{\mathbf{j}l} - \frac{1}{2}\right) - \mu\sum_{\mathbf{j}l\sigma} n^\sigma_{\mathbf{j}l}\ , \qquad (1)$$

describes a two-dimensional square lattice with electronic bands $l = d$ and $l = f$. The coordinates $(\mathbf{j}\,l)$ label the spatial site and band, respectively; $\sigma \in \{\uparrow,\downarrow\}$ denotes the spin of the electron. The operators $c_{\mathbf{j}l\sigma}$, $c^\dagger_{\mathbf{j}l\sigma}$, and $n^\sigma_{\mathbf{j}l} = c^\dagger_{\mathbf{j}l\sigma}c_{\mathbf{j}l\sigma}$ are the destruction, creation, and number operators. The first terms are the intraband and interband kinetic energies. The nearest-neighbor hopping matrix element in the d band will be chosen to be the unit of energy in the remainder of this work, $t_d = 1$, while its f-band counterpart, t_f, will be allowed to vary in the range $[-1.2,1.2]$. Because properties at V and $-V$ are related by the transformation $c_{id\sigma} \to -c_{id\sigma}$, we restrict the range of studied V to only positive values. The on-site repulsion U_l is chosen to be constant within a band: the f band will include a moderate interaction $U_f \equiv U = 4$ (unless otherwise mentioned), while the d band will be noninteracting $U_d = 0$. The chemical potential μ is set to zero, the system being then at commensurate filling for both $l = d, f$. This choice emphasizes Mott and antiferromagnetic physics and also avoids any sign problem in our DQMC simulations.

In the noninteracting limit $U = 0$, the regions with positive and negative t_f have quite distinct behaviors. The former is a metal with two overlapping bands, up to a critical interband hybridization above which it crosses into a band insulator, while the latter is always a band insulator. Such behavior is easily understood in terms of the dispersion and ensuing crossing of the independent f and d bands and is illustrated in the main panel of Fig. 1 for a one-dimensional geometry. More specifically, setting $x(k) = \cos k_x + \cos k_y$ gives band energies of the form

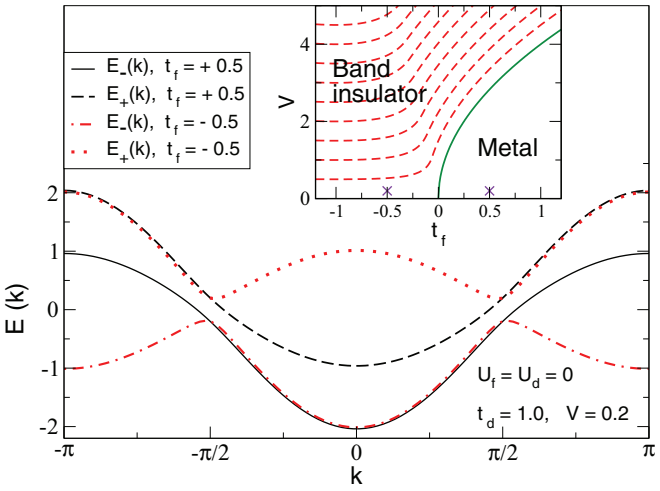

FIG. 1. (Color online) The one-dimensional $U_l = 0$ band structure [Eq. (2) with $\cos k_y = 0$], illustrating the distinct behavior of the two cases when t_d and t_f have the same sign and when they have the opposite sign. In the former situation, there are two overlapping bands as long as the interband hopping V is not too large, and the half-filled system is a metal. In the latter case, a gap opens between the bands, and the system is an insulator at half filling for all V. The inset shows the noninteracting phase diagram in two dimensions. Dashed lines are isolines at integer values of the gap.

$$E^0_\pm(x) = -(1+t_f)x \pm \sqrt{(1-t_f)^2x^2 + V^2}, \qquad (2)$$

with a metal-insulator transition at $|V| = 4\sqrt{t_f}$. Because there is perfect (π,π) nesting between the two branches of the Fermi surface, the metal is expected to develop long-range magnetic order at $T = 0$ and for arbitrarily weak repulsion. On the other hand, the presence of a gap in the band insulator implies that a finite U is required for the system to develop AF order. The gap is given by $\Delta = 2E^0_+(2)$ when $t_f > 0$ or when $V(1+t_f) > 4\sqrt{-t_f}(1-t_f)$ and $t_f < 0$ and by $\Delta = 4V\sqrt{-t_f}/|1-t_f|$ in all remaining cases of interest in the paper.

A. Mean-field theory

We use the conventional decoupling of the on-site interaction $Un^\uparrow n^\downarrow \to U(n_\uparrow\langle n_\downarrow\rangle + \langle n_\uparrow\rangle n_\downarrow - \langle n_\uparrow\rangle\langle n_\downarrow\rangle)$ with ansatz

$$\langle n_{\mathbf{j}l\uparrow}\rangle + \langle n_{\mathbf{j}l\downarrow}\rangle = 1, \quad \langle n_{\mathbf{j}l\uparrow}\rangle - \langle n_{\mathbf{j}l\downarrow}\rangle = 2s_l. \qquad (3)$$

This suffices since, at half filling, we do not expect the occurrence of noncollinear or inhomogeneous phases. By introducing the mean-field eigenvalues of a single layer

$$E_{k\pm} = \pm\sqrt{\epsilon_k^2 + (Us)^2}, \qquad (4)$$

we can conveniently express those of the bilayer as

$$\lambda = \pm\tfrac{1}{2}\Big[E^2_{k,d} + E^2_{k,f} + 2V^2 \pm \sqrt{\left(E^2_{k,d} - E^2_{k,f}\right)^2 + 4V^2\mathcal{E}^2}\Big]^{1/2}, \qquad (5)$$

where we omitted the $\pm$ subscript (since $E_{k\pm}$ always enter as squares) and we defined

$$\mathcal{E}^2 = \left(\sum_l \epsilon_{k,l}\right)^2 + \left(\sum_l s_l U_l\right)^2. \quad (6)$$

It is easy to verify that when $s_f s_d < 0$ (interband antiferromagnetic order), the equation $\lambda = 0$ does not admit any real solution regardless of the value of k. This implies that, when order sets in, the Fermi surface is fully gapped.

B. Determinant quantum Monte Carlo

In this approach[39,40] the partition function is written as a path integral, and the interaction is decoupled through the introduction of a space- and imaginary-time-dependent auxiliary field. Sampling this field stochastically produces the exact physics of the underlying Hamiltonian on finite clusters, apart from statistical errors, which can be reduced by running the simulation longer, and "Trotter errors"[41] associated with the discretization of the inverse temperature β. These can be eliminated by extrapolation to zero-imaginary-time mesh size $\delta\tau$. Here we have set $\delta\tau = 1/(8t_d)$ and verified that our results are qualitatively unchanged when $\delta\tau$ is reduced.

The DQMC results we present are computed for lattices of $N = 8 \times 8$ sites and two bands. At various points of the phase diagram, we checked that larger clusters do not lead to qualitatively different results. In many cases our focus is on physics at short length scales, e.g., near-neighbor spin correlations, which converge rapidly with lattice size. Every data point was obtained by averaging several independent simulations performed over a set of four different boundary conditions, leading to a better sampling of the first Brillouin zone and thereby reducing finite-size effects.

We quantify magnetism by examining the average f-band spin correlations along one direction

$$\mathcal{C}_{\mathbf{j}}(\mathbf{r}) \equiv \tfrac{1}{3}\langle \vec{\sigma}_{\mathbf{j}\,f} \cdot \vec{\sigma}_{\mathbf{j}+\mathbf{r},f}\rangle, \quad (7)$$

with $\sigma^z = c^\dagger_\uparrow c_\uparrow - c^\dagger_\downarrow c_\downarrow$, $\sigma^+ = 2c^\dagger_\uparrow c_\downarrow$, and $\sigma^- = 2c^\dagger_\downarrow c_\uparrow$. We use $\mathcal{C}_{\mathbf{j}}(\mathbf{r})$, rather than $\langle \sigma^z_{\mathbf{j}\,f}\sigma^z_{\mathbf{j}+\mathbf{r},f}\rangle$, because the Monte Carlo estimate of the former has a significantly smaller statistical uncertainty as a consequence of an anticorrelation of the deviations from the mean of measurements in the different spatial directions.

III. MAGNETIC CORRELATIONS

The on-site repulsion U favors localization of electrons by impeding double occupancy. We study this tendency by showing the local moments in the f band

$$m_f^2 \equiv \frac{1}{N}\sum_{\mathbf{j}} \mathcal{C}_{\mathbf{j}}(0)$$

in Fig. 2. In mean-field theory $m_f^2 = \frac{1}{2} + 2s_f^2$. The most obvious general trend is that localization decreases upon increasing the magnitude of either the f-band hopping t_f or the interband hybridization V. This observation, of course, reflects the competition between kinetic-energy scales and on-site repulsion U. As expected, the MFT local moment vanishes much more abruptly than its quantum Monte Carlo (QMC) counterpart, reflecting the fact that the moment can act as an order parameter within MFT.

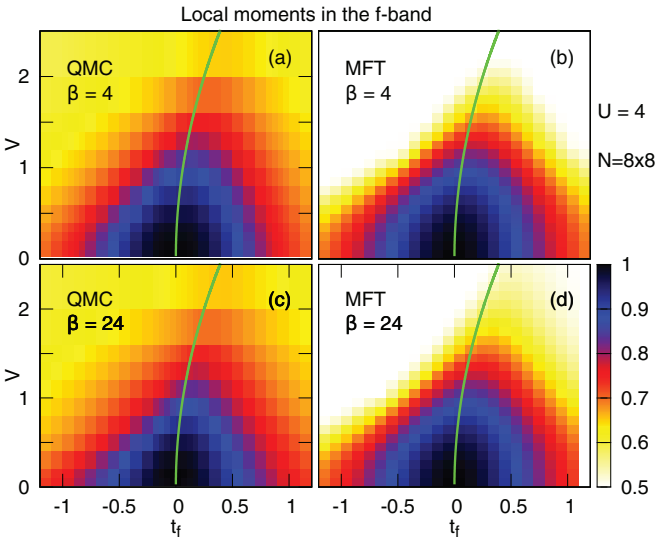

FIG. 2. (Color online) Evolution of the f-band local moment m_f^2 with t_f and V at $U = 4$ obtained by (left) QMC and (right) MFT. At $\beta = 4$ (top panels), the moments are mostly formed, and decreasing the temperature to $\beta = 24$ has no significant effect. m_f^2 is largest for small values of these two terms since this minimizes the quantum fluctuations. The curve extending upwards from the origin $(t_f, V) = (0,0)$ is the noninteracting ($U = 0$) band insulator to metal transition line. In the U nonzero case, m_f is best formed along this line.

We can understand the shape of the local moment dome from a weak-coupling perspective in three simple steps. (1) At $T = 0$ and for very weak interaction strengths, the diverging susceptibility implies that order must exist in the part of the $t_f - V$ plane where the noninteracting system is metallic: the dome would coincide precisely with the region to the right of the green line in the figures. (2) Finite U values at $T = 0$ cause the insulating phase to gradually order. In particular, the gap Δ decreases as V is decreased at constant t_f (see isolines in Fig. 1), and a transition to an ordered phase happens when $\Delta \propto U$, i.e., the dome described in step 1 acquires a tail in the negative t_f region. The larger U is, the thicker the tail becomes. (3) At a finite T, this picture needs to be modified to take into account that order will persist in a given region only up to a temperature of the order of the $T = 0$ AF gap. Because the gap is smallest in the region of large and positive V and t_f, such a region is also the first to lose order as the temperature is raised. These three arguments rationalize the shape of the moment dome in the t_f-V plane, its asymmetry with respect to the $t_f = 0$ axis, and its apex at positive t_f. In particular, this asymmetry in the values of m_f^2 implies that a small positive hopping t_f tends to strengthen the moment, while a small negative one tends to weaken it.

In regimes where a weak-coupling treatment is appropriate, i.e., when moments are small, these arguments carry through to the staggered magnetization and, as a direct consequence, to long-range correlations (although, because the system is two-dimensional, the former is only different from zero at $T = 0$). We quantify the evolution of long-range (l.r.) correlations by

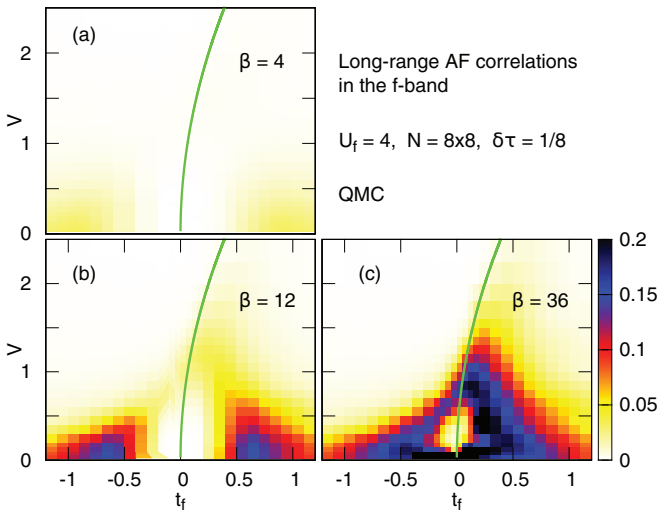

FIG. 3. (Color online) The f-band long-range antiferromagnetic correlations $\mathcal{C}_{\text{l.r.}}$, shown in the t_f-V plane for different inverse temperatures β. Because $\mathcal{C}_{\text{l.r.}}$ probes spin ordering at large distance, the convergence with increasing β is more gradual than for the local moments. As β increases, in the paramagnetic region where V and t_f are both small, the AF energy scales are also too small, and AF order is absent. This region shrinks as β increases and the temperature systematically falls below the AF energy scales. As with the local moment, $\mathcal{C}_{\text{l.r.}}$ is peaked at small positive t_f. The green curve is the noninteracting metal-insulator transition line.

looking at

$$\mathcal{C}_{\text{l.r.}} \equiv \frac{1}{N'N} \sum_{\mathbf{j}} {\sum_{\mathbf{r}}}' \mathcal{C}_{\mathbf{j}}(\mathbf{r})(-1)^{|x+y|}. \tag{8}$$

The prime symbols in the sum and in the number of sites N' indicate that we omitted contributions from local and nearest-neighbor correlations in order to better single out the long-range behavior.[42] For large cluster sizes, $N\mathcal{C}_{\text{l.r.}}$ converges to the f-band antiferromagnetic structure factor. As shown in Fig. 3, $\mathcal{C}_{\text{l.r.}}$ defines a dome with the same characteristic asymmetry as that of the moments but whose edge is more sharply defined, reminiscent of the behavior of an order parameter.

At strong coupling, where U is large and both t_f and V are small, the weak-coupling picture needs to be modified in favor of one where the local moments are fully formed and interact with conducting electrons and each other via, respectively, exchange couplings $J_\perp \propto V^2/U$ and $J \propto t_f^2/U$. To develop long-range correlations in these regimes one needs to get down to temperatures of the order of J and $J_\perp$, and this, in turn, leads to the persistence of an area inside the dome where long-range correlations have still not developed at the lowest T we considered.

Having described the behavior of the local moment (Fig. 2) and long-range correlations (Fig. 3), we now turn to near-neighbor (n.n.) correlations (Fig. 4)

$$\mathcal{C}_{\text{n.n.}} \equiv \frac{1}{N} \sum_{\mathbf{j}} |\mathcal{C}_{\mathbf{j}}(1,0)|. \tag{9}$$

One naturally expects the dome of n.n. correlations to resemble the one of longer-range correlations; that is, for a given temperature, regions with large n.n. spin correlations correspond to regions with large long-range correlations. One would also expect near-neighbor correlations to be always significantly larger than longer-range correlations, rather independent of temperature, and, in fact, much larger at high T where long-range correlations are exponentially small. Although these expectations are satisfied in much of the t_f-V plane and at low T (Fig. 4), our results indicate that the finite-T scenario as the metallic phase is entered is of less straightforward interpretation.

We can more precisely illustrate the anomalous behavior of the n.n. correlations along the metal-insulator line by looking at the evolution of short- and long-range correlations for constant V as t_f is varied (Fig. 5). For instance, at $V = 0.8$ and $\beta = 12$, both correlations show a minimum after the metal-insulator line is crossed. As the temperature is decreased to $\beta = 36$ and in proximity to the same value of t_f, longer-range correlations have developed a peak, while the n.n. ones still show a dip. At this low temperature, both correlations are of essentially equal magnitude. This is the rather generic behavior found in correspondence to crossing the metallic line (see $V = 1.2$ in Fig. 5), which contradicts both expectations above.

It is impossible to attribute this effect to the f-intralayer exchange coupling because the latter is too small and the temperature too high. Instead, the correlation between the position of the peak and the metal-insulator line suggests that the change brought by t_f must be related to the fact that the underlying noninteracting system develops a Fermi surface. Although this is beneficial to both RKKY interaction and Kondo screening, it is hard to reconcile our results with a scenario where the Kondo effect is important since screening of the local moments should cause a rather uniform decrease of spin correlations irrespective of the distance.

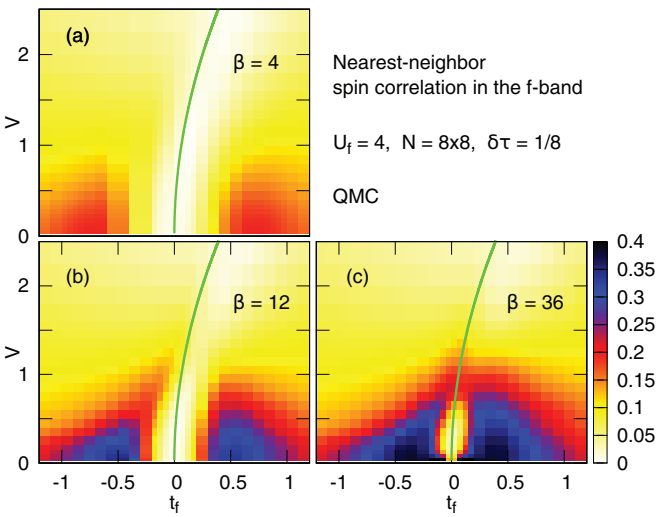

FIG. 4. (Color online) Near-neighbor spin correlations in the f band $\mathcal{C}_{\text{n.n.}}$. t_f provides an exchange interaction $J = 4t_f^2/U$ in the f band, which leads to antiferromagnetic correlations. V also causes antiferromagnetic interactions via RKKY coupling. There is significant growth in the spin correlations as β increases, even well after the local moment has saturated (Fig. 2). The $U = 0$ band insulator to metal transition line is characterized by reduced values of the near-neighbor spin correlations.

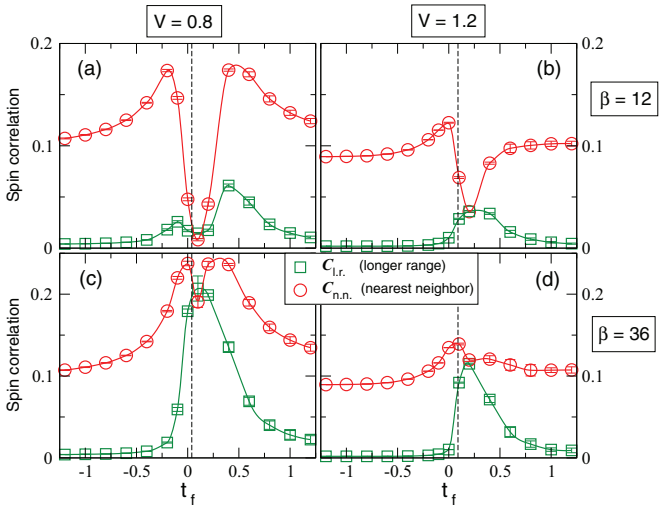

FIG. 5. (Color online) Comparison between near-neighbor, $\mathcal{C}_{\text{n.n.}}$, and long-range, $\mathcal{C}_{\text{l.r.}}$, correlations. Results are shown as functions of t_f for two values of the hybridization, $V = 0.8, 1.2$, and at two distinct temperatures, $\beta = 12, 36$. The dashed lines indicate the metal-insulator transition in the noninteracting case and closely track the downturn of the magnitude of n.n. spin correlation.

The drop in n.n. correlations likely indicates a weaker effective spin-spin interaction at the metal-insulator line than in neighboring regions of the t_f-V plane. At the same time, though, the peak in longer-range correlations and the fact that their magnitude is identical to the n.n. one suggest that the range of the effective spin-spin interaction is longer in the proximity of the metal-insulator line than at any other value of t_f.

IV. DENSITY OF STATES

The spectrum of excitations of the PAM at half filling displays complex features reflecting the interplay of antiferromagnetic order, the formation of a Mott insulator, and the emergence of Kondo singlets. The former two effects suppress the density of states at the Fermi level, giving rise to "Slater" and "Mott" gaps, respectively. The latter causes screening of the local moments in the f band and is associated with a Kondo resonance (peak) at the Fermi level. The temperature affects these competing possibilities. For example, a Kondo resonance might first form as T is lowered, followed by a splitting of that resonance as magnetic correlations grow. In addition to these correlation effects, the spectral function is also influenced by the character of the noninteracting band structure and, in particular, by whether or not the system is metallic.

We explore these issues by extracting the single-particle excitation spectrum $A_f(\omega)$ via analytic continuation of the local time-dependent Green's function $G_f(\tau) = \langle c_i(\tau) c_i^\dagger(0)\rangle$ measured in QMC simulations. This involves the inversion of the relation

$$G_f(\tau) = \int_{-\infty}^{+\infty} d\,\omega\, \frac{e^{-\omega\tau}}{1+e^{-\beta\omega}}\, A_f(\omega), \tag{10}$$

which we perform using the maximum entropy method.[43,44]

We begin with the spectra at inverse temperature $\beta = 2$, which is cold enough to have allowed for some of the many-body physics to have occurred, e.g., moment formation and moment screening, but not sufficiently cold for spin correlations to have attained their ground-state values (see Figs. 3 and 4). Figure 6 shows the density of states in the f band as a function of the interband hybridization V at two values of on-site repulsion, $U = 4$ (upper panels) and $U = 8$ (lower panels). Results for four values of the hopping parameter in the

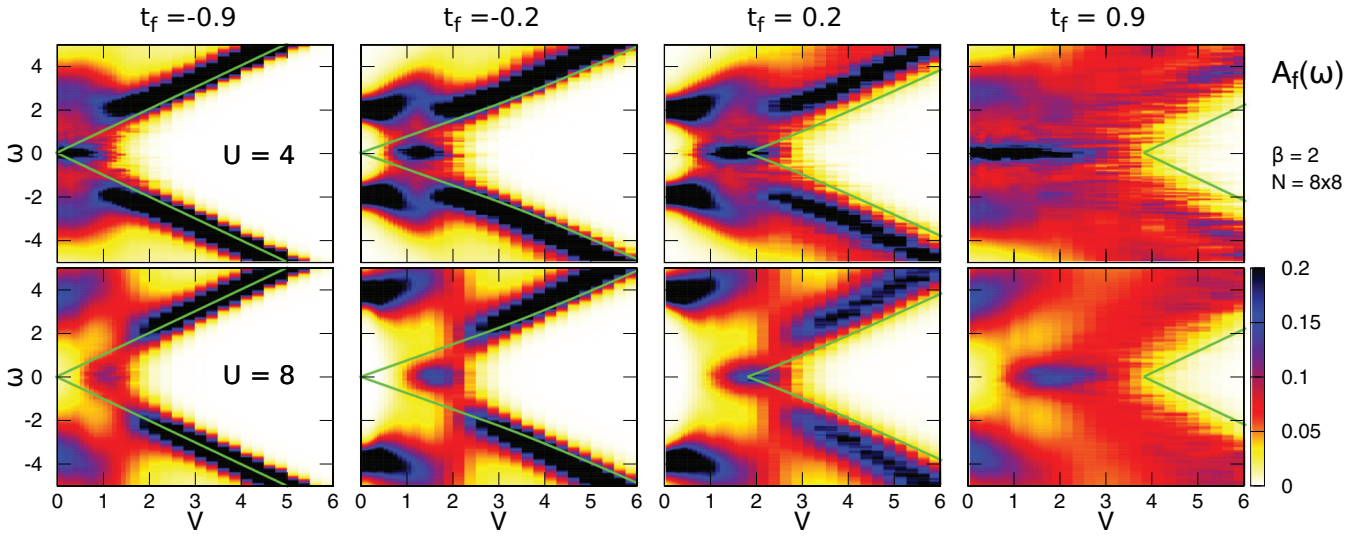

FIG. 6. (Color online) The spectrum of the f band at $U = 4, 8$ (top and bottom, respectively) as a function of interband hybridization V for inverse temperature $\beta = 2$. Four values of f-band hopping t_f are shown. At small V, two bands are separated by a Slater gap of width U, corresponding to the cost of double occupancy. The Kondo resonance is visible at $\omega = 0$ for V below a critical threshold V_c. The triangular-shaped regions at large V correspond to the singlet formation that prevents Kondo resonance and leads to a gap that is well described by the noninteracting dispersion relation. The green lines correspond to the edges of the noninteracting density of states, which delimit the band gap.

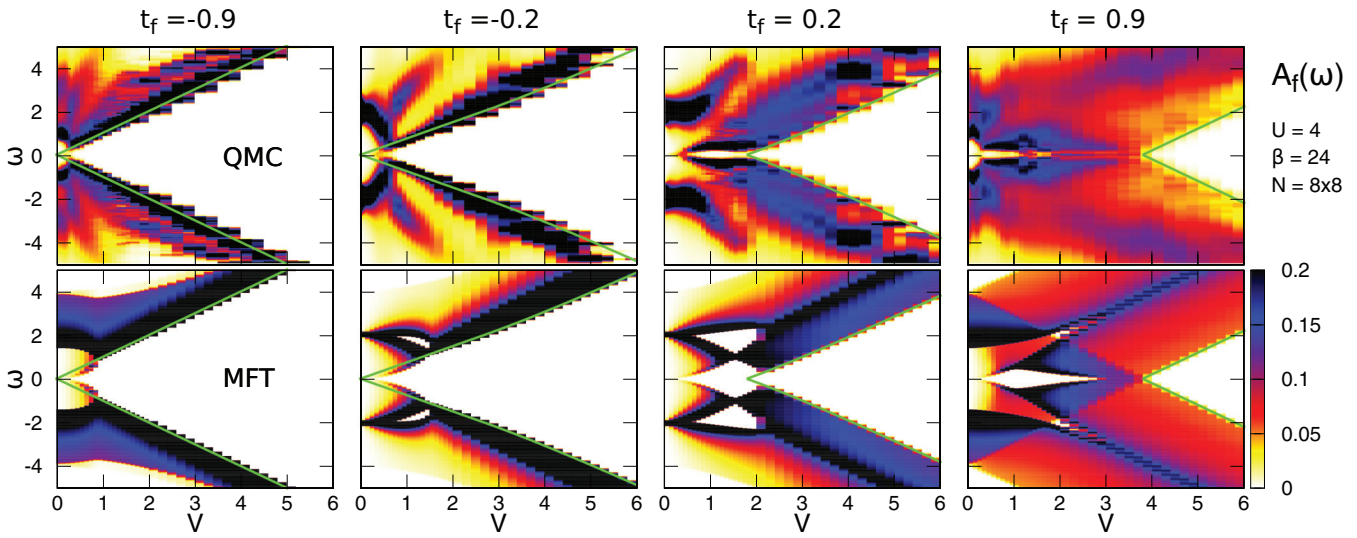

FIG. 7. (Color online) The upper panels are the same as Fig. 6, except at much lower temperature $\beta = 24$. The smearing of the band gaps is greatly reduced. In addition the Kondo resonance has been split by a gap associated with the formation of AF order. The insulating character of the $t_f < 0$ case for all V is more apparent at this lower temperature. We show only $U = 4$, with QMC in the top panels and MFT in the bottom ones. The green lines delimit the noninteracting band gap.

correlated band, $t_f \in \{-0.9, -0.2, +0.2, +0.9\}$, are given. In green we plot the edges of the noninteracting bands, defined by Max$[E^0_-(\mathbf{k})]$ and Min$[E^0_+(\mathbf{k})]$, which delimit the band gap at $U = 0$.

For $t_f = \pm 0.9$ and $U = 4$ the density of states has a peak at small V which extends all the way down to $V = 0$. The peak is absent at $U = 8$, where a fully formed Mott gap appears as V approaches zero. Both points indicate that $\beta = 2$ is too high a temperature for moment formation and Mott-insulating behavior to develop at $U = 4$. On the other hand, at $U = 4$ and $t_f = \pm 0.2$, moments have formed, and the $\omega = 0$ feature that develops at finite V is a Kondo resonance. The situation at $U = 8$ differs because, as already remarked, the $V = 0$ system is a Mott insulator (in the f band) even at $t_f = \pm 0.9$. Hence we see clear signs of broad Kondo resonances at intermediate V for all four values of t_f.

While in the case of negative t_f the noninteracting limit is always gapped, in the case of positive t_f there is a critical V for insulating behavior, leading to a larger region of the phase space in which low-energy excitations allow Kondo physics to occur down to low temperatures. Alternatively put, the gapped single-particle density of states characteristic of negative t_f freezes the electrons and prevents screening of the f moments. This causes a marked difference between the spectrum at positive and negative values of t_f at low temperature. Consider the cases of $t_f = \pm 0.2$ and $\beta = 24$ reported in Fig. 7. One immediately sees that the sharp feature present at higher T has survived for $t_f = 0.2$, albeit split as the result of the particular filling considered and the onset of magnetic correlations. In contrast, $t_f = -0.2$ shows no signature of the Kondo resonance that appears at higher T.

It is also instructive to compare the QMC results with mean-field theory (Fig. 7). We observe that at the low temperature presently considered, most of the features of the spectrum are reproduced by the mean-field solution. At $t_f = 0.2$ and $V < 2$, however, the mean-field gap has a more pronounced dependence on V, and it is visibly larger. We attribute both differences to the fact that DQMC describes a Kondo insulator, with a gap forming on top of the Kondo resonance, while mean-field theory, by its very nature, describes a Slater insulator and has no possibility to access the physics of Kondo screening.

The particular way of representing the data makes also quite clear the value of V where one can identify the onset of band-insulating behavior: a main feature visible in each of the panels is the transition to a regime where the gap opens linearly as V increases and whose width is consistent with the noninteracting expressions. We found that for $t_f > 0$, the onset of band-insulating behavior happens at roughly the same value of V in both mean-field theory and QMC. For $t_f < 0$, there is a closing of the gap as the value of V is initially increased, so that one can identify the onset of band-insulating behavior when this trend is reversed and the gap opens up as V further increases. We found, especially clearly at $t_f = -0.9$, that the value of V at which such Mott-to-band insulator "transition" occurs is severely overestimated by mean-field theory.

V. CONCLUSIONS

In this paper we have used mean-field theory and the determinant quantum Monte Carlo method to explore systematically the effect of f-orbital bandwidth in a two-band Hubbard Hamiltonian. These data expand upon the more well-studied cases when $t_f = 0$ (the periodic Anderson model) and $t_f = t_d$ (the Hubbard bilayer). In addition, we have obtained data for t_f of opposite sign to t_d. Our work quantifies the role that shifts in the overlap of localized orbitals on neighboring atoms might play in the mechanism whereby pressure destroys AF correlations in heavy-fermion and transition-metal-oxide materials.

One key conclusion of our work is that magnetic correlations are maximized for small positive t_f, in correspondence to where the noninteracting system becomes metallic. We found that nearest-neighbor correlations show very peculiar behavior and are, in fact, suppressed in the optimal regime for observing long-range order. We can only reconcile this surprising behavior as a signature that the effective spin-spin interaction at the metal-insulator line is weaker than in neighboring regions but has a longer range than for any other value of t_f.

Finally, the study of the single-particle spectral function reveals that tuning the f bandwidth deeply modifies the low-energy spectrum of this model. In contradiction to what was found in a previous study,[23] the Coulomb interaction does not simply lead to the renormalization of the noninteracting properties. While certain of the qualitative features of the spectra can be well understood from the mean-field and noninteracting band structure, other features suggest more subtle correlation physics. In particular, at fairly high temperature a Kondo resonance can develop at both positive and negative t_f values, while at low temperature only positive t_f shows the presence of a split Kondo resonance.

ACKNOWLEDGMENTS

S.C. and R.T.S. acknowledge support, respectively, from the DOE (Grant No. DE-SC0008627) and from the laboratory collaboration funding from the University of California, Office of the President. This work was also supported by the CNRS–UC Davis EPOCAL LIA joint research grant and by the NNSA under Project No. 201223433.

[1] M. Rasetti, *The Hubbard Model: Recent Results* (World Scientific, Singapore, 1991).
[2] *The Hubbard Model*, edited by A. Montorsi (World Scientific, Singapore, 1992).
[3] F. Gebhard, *The Mott Metal-Insulator Transition, Models and Methods* (Springer, New York, 1997).
[4] P. Fazekas, *Lecture Notes on Electron Correlation and Magnetism* (World Scientific, Singapore, 1999).
[5] J. Zaanen and O. Gunnarsson, Phys. Rev. B **40**, 7391 (1989).
[6] K. Machida, Phys. C **158**, 192 (1989).
[7] M. Kato, K. Machida, H. Nakanishi, and M. Fujita, J. Phys. Soc. Jpn. **59**, 1047 (1990).
[8] M. Inui and P. B. Littlewood, Phys. Rev. B **44**, 4415 (1991).
[9] J. Yang and W. P. Su, Phys. Rev. B **44**, 6838 (1991).
[10] D. J. Scalapino, in *Proceedings of the International School of Physics*, edited by R. A. Broglia and J. R. Schrieffer (North-Holland, New York, 1994), pp. 95–125, and references cited therein.
[11] I. Sugitani, Y. Okuda, H. Shishido, T. Yamada, A. Thamizhavel, E. Yamamoto, T. D. Matsuda, Y. Haga, T. Takeuchi, R. Settai, and Y. Onuki, J. Phys. Soc. Jpn. **75**, 043703 (2006).
[12] G. R. Stewart, Rev. Mod. Phys. **73**, 797 (2001).
[13] A. Georges, G. Kotliar, W. Krauth, and M. J. Rozenberg, Rev. Mod. Phys. **68**, 13 (1996).
[14] D. Vollhardt, in *Correlated Electron Systems*, edited by V. J. Emery (World Scientific, Singapore, 1993), p. 57; Th. Pruschke, M. Jarrell, and J. K. Freericks, Adv. Phys. **44**, 187 (1995).
[15] M. Ulmke, R. T. Scalettar, A. Nazarenko, and E. Dagotto, Phys. Rev. B **54**, 16523 (1996).
[16] K. Held, C. Huscroft, R. T. Scalettar, and A. K. McMahan, Phys. Rev. Lett. **85**, 373 (2000).
[17] R. T. Scalettar, J. W. Cannon, D. J. Scalapino, and R. L. Sugar, Phys. Rev. B **50**, 13419 (1994).
[18] A. W. Sandvik and D. J. Scalapino, Phys. Rev. Lett. **72**, 2777 (1994).
[19] S. R. White, Phys. Rev. Lett. **69**, 2863 (1992); Phys. Rev. B **48**, 10345 (1993); S. R. White and D. J. Scalapino, Phys. Rev. Lett. **80**, 1272 (1998); **81**, 3227 (1998).
[20] M. Vekic, J. W. Cannon, D. J. Scalapino, R. T. Scalettar, and R. L. Sugar, Phys. Rev. Lett. **74**, 2367 (1995).
[21] A. Toropova, C. A. Marianetti, K. Haule, and G. Kotliar, Phys. Rev. B **76**, 155126 (2007).
[22] M. A. Continentino, G. M. Japiassu, and A. Troper, Phys. Rev. B **49**, 4432 (1994).
[23] Y. Shimizu, O. Sakai, and A. C. Hewson, J. Phys. Soc. Jpn. **69**, 1777 (2000).
[24] O. Sakai, Y. Shimizu, and Y. Kaneta, J. Phys. Soc. Jpn. **74**, 2517 (2005).
[25] L. de' Medici, A. Georges, G. Kotliar, and S. Biermann, Phys. Rev. Lett. **95**, 066402 (2005).
[26] T. Yoshida, T. Ohashi, and N. Kawakami, J. Phys. Soc. Jpn. **80**, 064710 (2011).
[27] A. Liebsch, Phys. Rev. B **70**, 165103 (2004).
[28] A. Liebsch, Phys. Rev. Lett. **95**, 116402 (2005).
[29] R. Arita and K. Held, Phys. Rev. B **72**, 201102(R) (2005).
[30] K. Inaba and A. Koga, Phys. Rev. B **73**, 155106 (2006).
[31] T. A. Costi and A. Liebsch, Phys. Rev. Lett. **99**, 236404 (2007).
[32] A. Koga, N. Kawakami, T. M. Rice, and M. Sigrist, Phys. Rev. Lett. **92**, 216402 (2004).
[33] M. Ferrero, F. Becca, M. Fabrizio, and M. Capone, Phys. Rev. B **72**, 205126 (2005).
[34] L. de'Medici, A. Georges, and S. Biermann, Phys. Rev. B **72**, 205124 (2005).
[35] A. Ruegg, M. Indergand, S. Pilgram, and M. Sigrist, Eur. Phys. J. B **48**, 55 (2005).
[36] K. Inaba, A. Koga, S.-I. Suga, and N. Kawakami, Phys. Rev. B **72**, 085112 (2005).
[37] C. Knecht, N. Blumer, and P. G. J. van Dongen, Phys. Rev. B **72**, 081103(R) (2005).
[38] S. Biermann, L. de'Medici, and A. Georges, Phys. Rev. Lett. **95**, 206401 (2005).
[39] R. Blankenbecler, D. J. Scalapino, and R. L. Sugar, Phys. Rev. D **24**, 2278 (1981).
[40] S. R. White, D. J. Scalapino, R. L. Sugar, E. Y. Loh, Jr., J. E. Gubernatis, and R. T. Scalettar, Phys. Rev. B **40**, 506 (1989).
[41] H. F. Trotter, Proc. Am. Math. Soc. **10**, 545 (1959); M. Suzuki, Prog. Theor. Phys. **56**, 1454 (1976); R. M. Fye, Phys. Rev. B **33**, 6271 (1986); R. M. Fye and R. T. Scalettar, *ibid.* **36**, 3833 (1987).
[42] C. N. Varney, C. R. Lee, Z. J. Bai, S. Chiesa, M. Jarrell, and R. T. Scalettar, Phys. Rev. B **80**, 075116 (2009).
[43] J. E. Gubernatis, M. Jarrell, R. N. Silver, and D. S. Sivia, Phys. Rev. B **44**, 6011 (1991).
[44] K. S. D. Beach, arXiv:cond-mat/0403055.